TÉCNICO LISBOA

Helping cells jump to conclusions.

Design and implementation of a biological circuit capable of responding to pre-equilibrium information.

Andreas Constantinou

Thesis to obtain the Master of Science Degree in

Biotechnology

Supervisors: Prof. Dr. Miguel Nobre Parreira Cacho Teixeira
Prof. Dr. Alejandro Colman-Lerner

Examination Committee

Chairperson:	Prof. Dr. Isabel Maria de Sá-Correia Leite de Almeida
Supervisor:	Prof. Dr. Miguel Nobre Parreira Cacho Teixeira
Member of the Committee:	Prof. Dr. Pedro Tiago Gonçalves Monteiro

October 2014

Acknowledgements

Thanks to Professor Alejandro Colman-Lerner and Dr. Alejandra Ventura for offering me this master's thesis project and for their unconditional support throughout the entire project. It has been a fantastic and inspiring experience for me, that has certainly resparked my interest for science and research.

Furthermore, thanks to Professor Miguel Teixeira, Professor Juho Rousu, Professor Erik Aurell, Professor Isabel Sá-Correia, Karin Knutsson, Päivi Koivunen, Instituto Superior Técnico, Aalto University, Royal Institute of Technology, University of Buenos Aires, the European Commission, and all other contributors for making this master's thesis and my studies at the euSYSBIO Erasmus Mundus program possible.

Also, to my parents, Fabian Rudolf, Tiago Ferreira, Lorena Bolaños, Jacek Dąbrowski, Siavash Laghai, Gonçalo Pestana, Siniša Matetić, my friends in the ACL lab and at IFIBYNE, my dear 4.40's, my euSYSBIO mates, Elisabeth Haggård, and all the other people who inspired, helped, supported, and motivated me during this journey:

Thank you, tack, ευχαριστώ, gracias, obrigado, and danke!

I would not have made it here and it definitely would not have been the same without you. Forever indebted and grateful...

Buenos Aires, October 27, 2014

Andreas Constantinou

Resumo

Muitos processos celulares dependem da capacidade das células responderem à informação química do ambiente que as rodeia. As células têm esta capacidade por utilizar proteínas receptoras que se ligam aos sinais químicos (ligandos), convertendo essa informação química em sinais intracelulares a que as células podem responder. Para além disso, diferentes concentrações de ligando podem ser diferenciadas pela razão receptores ligados versus desligados. Embora isto seja geralmente possível apenas para concentrações que não saturem os receptores, foi demonstrado recentemente que a capacidade de distinguir diferentes concentrações de ligando pode, em teoria, ser extendida à gama de saturação, pela utilização da informação pré-equilíbrio, resultante da cinética de ligação ligando–receptor. Este mecanismo foi denominado *pre-equilibrium sensing and signaling* (PrESS). Neste trabalho, investigou-se a possibilidade de implementar biologicamente esta ideia, como um circuito genético controlável e simples. Por meio de modelação computacional e de experimentação laboratorial verificou-se que a repressão baseada num sensor, auxiliada pelo influxo lento de um ligando, gera uma dinâmica de pré-equilíbrio que pode permitir às células distinguir entre diferentes concentrações saturantes de ligando. Contudo, a dinâmica observada difere da originalmente descrita como PrESS, tornando o sistema menos geral. Possíveis modificações que levam à geração de uma dinâmica mais semelhante à PrESS são, por isso, discutidas.

Palavras-chave: cinética de ligação, sinalização celular, cinética pré-equilíbrio, biologia de sistemas

Abstract

Many cellular processes rely on the ability of cells to sense and respond to chemical information in their immediate surroundings. Cells can achieve this by binding chemical signals (ligand) to specific receptor proteins, that convert the chemical information into intracellular signals to which the cells can respond. Furthermore, different concentrations of ligand may be distinguished by the fraction of bound to unbound receptor. Although this is generally only possible for concentrations that do not saturate the receptors, it was recently shown that cells' ability to distinguish between ligand concentrations could in theory be expanded into the saturating range, by the utilization of pre-equilibrium information resulting from the ligand–receptor binding kinetics. This mechanism was termed pre-equilibrium sensing and signaling (PrESS). Here, the possibility to biologically implement this idea as a simple, controllable genetic circuit is investigated. Via computational modeling and experiments it is shown that repression-based sensing, aided by slow influx of ligand, generates pre-equilibrium dynamics that may enable cells to distinguish between different saturating concentrations of ligand. However, these dynamics differ from those originally described for PrESS, making the system less general. Potential modifications to generate more PrESS-like dynamics are therefore also discussed.

Keywords: binding kinetics, cell signaling, pre-equilibrium kinetics, systems biology

Contents

Abbreviations and Acronyms

PrESS	Pre-equlibrium sensing and signaling
SGR	Yeast growth medium
TF	Transcription factor

Chapter 1

Introduction

Making the first im*press*ion count

Cells from all domains of life have evolved strategies for responding to changes in their immediate surroundings. For example, through processes collectively known as signal transduction, cells are able to sense and transmit extracellular information into the cell interior, allowing a cellular response without requiring physical entry of the signal in question (Gomperts et al., 2009; Stock et al., 2000).

1.1 Signal transduction

A typical example of a signal transduction system involves binding of extracellular molecules, or ligands, to ligand-specific receptors present on the cell surface. These receptors are generally proteins integrated into the plasma membrane, protruding to both the interior and the exterior of the cell. Binding of ligand may induce a conformational change in the receptor, thereby transforming it from an inactive form to an activated ligand–receptor complex. Via intracellular domains, the activated receptor complex is able to bind and/or act on downstream cellular signal mediators, thereby converting the information received from the extracellular ligand into an intracellular signal to which the cell machinery is able to respond (Gomperts et al., 2009).

Although the exact response induced by a certain extracellular ligand may be a complex matter that depends on many additional factors, the magnitude of a response is often proportional to the fraction of receptors occupied by the ligand. This is known as the dose–response relationship, and can be visualized by plotting the measured response against increasing concentrations of ligand (figure 1.1) (Gomperts et al., 2009).

An obvious but important feature of the dose-response effect is the tendency towards a maximal response with increasing concentrations of ligand. Once the concentration of extracellular ligand is high enough to result in a near-complete receptor occupation, increasing the ligand concentration even further will not significantly increase the fraction of bound receptors. Therefore, when two saturating concentrations of ligand result in nearly equal fractions of bound receptor in equilibrium, the amount of signal transduced intracellularly by the activated receptors will be the same. I.e., different saturating

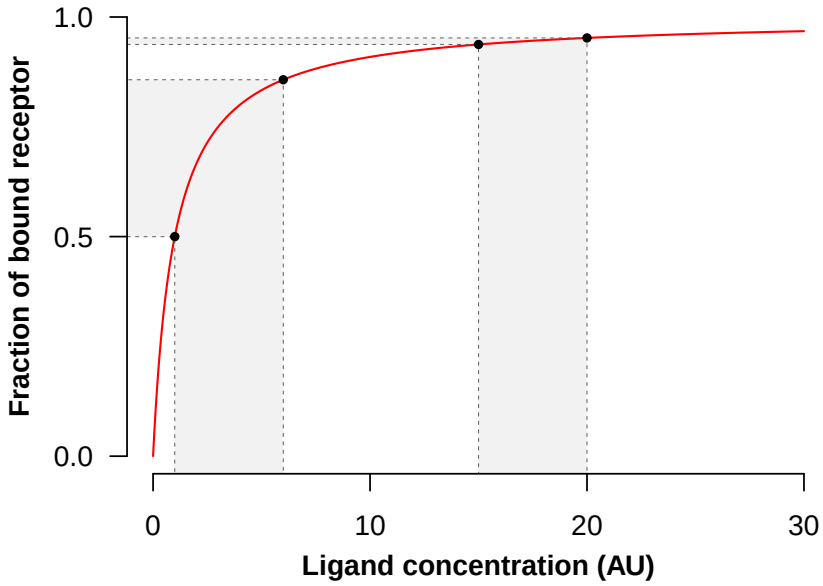

Figure 1.1: The dose–response relationship. A typical dose–response curve for a ligand–receptor binding reaction plotted in linear scale. At high levels of input almost all receptors are bound by ligand and the system gets saturated: increasing the ligand concentration even further does no longer significantly change the response.

levels of ligand will not be distinguishable by the cell once binding has reached equilibrium.

1.2 Pre-equilibrium sensing and signaling

While studying the pheromone signaling response of the budding yeast *Saccharomyces cerevisiae*, Ventura et al. (2014) proposed a mechanism which could potentially explain the cells' remarkable ability to distinguish between different saturating concentrations of mating pheromone (Segall, 1993; Moore et al., 2008). Briefly, their mechanism suggested that cells may take advantage of differences in pheromone receptor occupancy levels prior to the binding of pheromone reaches equilibrium, and has thus been termed pre-equilibrium sensing and signaling (PrESS) (Ventura et al., 2014).

The idea of PrESS can be explained by looking at the reaction kinetics of a simple ligand–receptor binding reaction such as that shown in figure 1.2. Free receptor molecules (R) in the plasma membrane are bound by receptor-specific ligands (L), forming an activated complex (C) which can signal to cellular components downstream of the receptor. In the reverse reaction, ligand molecules dissociate from the receptor, which returns the receptor to its inactive, non-signaling state. These reactions can be represented chemically by the reaction equation:

$$\mathrm{R} + \mathrm{L} \underset{k_{off}}{\overset{k_{on}}{\rightleftharpoons}} \mathrm{C} \qquad \text{(R 1.1)}$$

where R, L, and C represent free receptor, ligand, and ligand–receptor complex, respectively; and k_{on} and k_{off} are the reaction rate constants of the association and dissociation reactions. Using the law of mass-action, and assuming that ligand is in excess over receptor ($L \gg R$) so that the concentration of ligand is not significantly affected by the binding reaction, the reaction can be written mathematically as

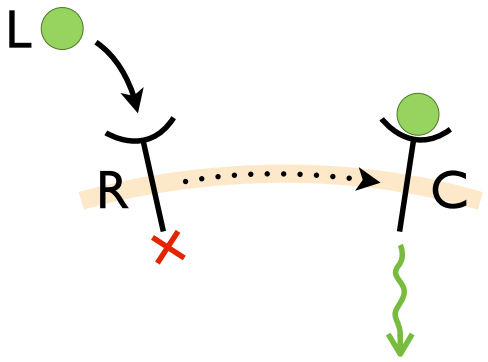

Figure 1.2: Example of a simple ligand–receptor binding and signaling system. Signaling from the ligand receptor (R) is inactive in the absence of ligand (L). Binding of ligand converts the receptor into its activated complex form (C), which can participate in downstream signaling.

a differential equation that describes the *net change* in complex formation over time:

$$\frac{d\mathrm{C}}{dt} = \mathrm{k_{on}LR} - \mathrm{k_{off}C}. \tag{1.1}$$

Prior to ligand stimulation (i.e., in the absence of ligand), all receptor molecules will be in their free form R, and equation 1.1 will be equal to zero. Once ligand is added to the system, reaction 1.1 will commence, initially with the forward reaction completely dominating. This will yield equation 1.1 positive, representing a net formation of complex C. As C begins to accumulate, the rate of the reverse reaction will increase accordingly, until eventually a new equilibrium is reached when the reaction rates of association and dissociation are equal, and equation 1.1 once again equals zero.

Assuming a conservation law for the receptor, $\mathrm{R_{tot}} = \mathrm{R} + \mathrm{C}$, equation 1.1 can be solved to reveal the *amount* of complex C formed over time t, given a specific concentration of ligand L, $\mathrm{C}_{(t,\mathrm{L})}$:

$$\mathrm{C}_{(t,\mathrm{L})} = \mathrm{C_{eq(L)}}\left(1 - e^{-t/\tau_{(\mathrm{L})}}\right), \tag{1.2}$$

where

$$\mathrm{C_{eq(L)}} = \mathrm{R_{tot}}\frac{\mathrm{L}}{\mathrm{L} + \mathrm{k_{off}}/\mathrm{k_{on}}} \tag{1.3}$$

is the amount of complex formed in equilibrium, and

$$\tau_{(L)} = \frac{1}{\mathrm{k_{off}} + \mathrm{k_{on}}\times\mathrm{L}} \tag{1.4}$$

defines the time constant of the reaction; it will be explained in a later section. $\mathrm{C_{eq(L)}}$ is readily derived from the steady state of equation 1.1. Equation 1.2 is visualized in figure 1.3, where the fraction of bound receptors is plotted over time following induction with a high concentration of ligand in relation to receptor.

To understand PrESS, it is important to note that the net reaction rate at different time points after the addition of ligand until the system reaches equilibrium will depend on the ligand concentration. More

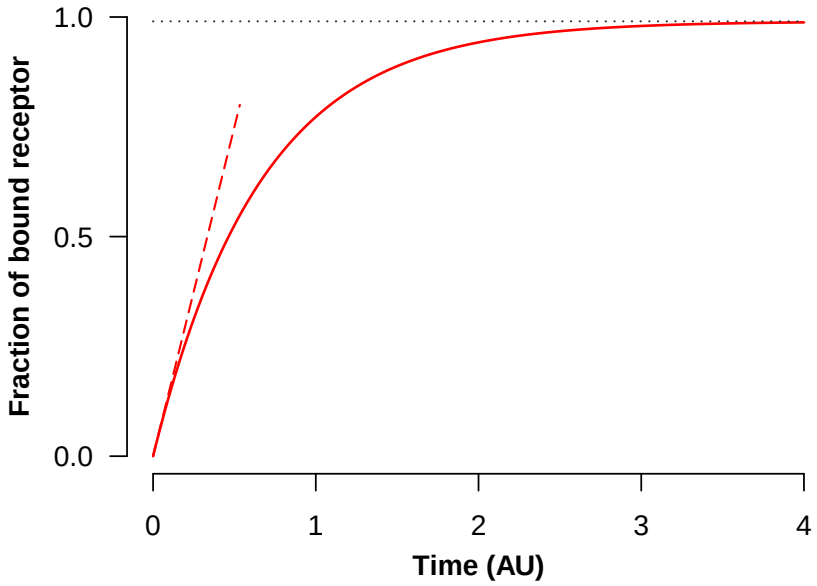

Figure 1.3: Receptor complex formation over time in response to a saturating ligand concentration. As the rate of association decreases with dropping numbers of free receptor, the dissociation reaction rate increases accordingly. This gives rise to the smooth approach of the curve to equilibrium. The slope of the dashed tangent line indicates the initial reaction rate at time $t = 0$. The dotted, horizontal line marks the level of complex in equilibrium.

specifically, although two saturating ligand concentrations may lead to nearly indistinguishable fractions of complex once the system reaches equilibrium, the amount of complex formed at different time points prior to equilibrium may still differ significantly. This is shown in figure 1.4, where the complex formation in response to two different concentrations of ligand is plotted over time. A higher ligand concentration (blue curve) gives rise to a faster initial accumulation of complex compared to a lower concentration (red curve). Although the two curves eventually reach nearly equal fractions of bound receptor, the initial difference in receptor binding rates opens a pre-equilibrium window where the amounts of formed complex differ greatly between the curves.

Given this situation, if cells were to respond to downstream signaling from ligand–receptor complex in equilibrium, they would have all but no information for discriminating between the two concentrations of ligand. However, if downstream signaling is fast enough to let cells respond to receptor signaling before the binding reaction has reached equilibrium, the two concentrations of ligand could potentially be differentiated. This is precisely the rational of PrESS.

1.2.1 PrESS requires that the response time is input dependent

The root to the pre-equilibrium dynamics in ligand–receptor binding lies in the association and dissociation rates. Since the association reaction is proportional to the concentration of the reactants, a higher ligand concentration initially leads to a faster accumulation of complex. In contrast, the dissociation reaction is proportional only to the concentration of complex, which has an upper limit in the total number of receptors, $\mathrm{R}_{\mathrm{tot}}$. As a result, increasing the ligand concentration increases the initial complex accumulation rate, which in turn means that the reaction will approach binding equilibrium faster.

This result is explained mathematically by the time constant τ (equation 1.4). The time constant is

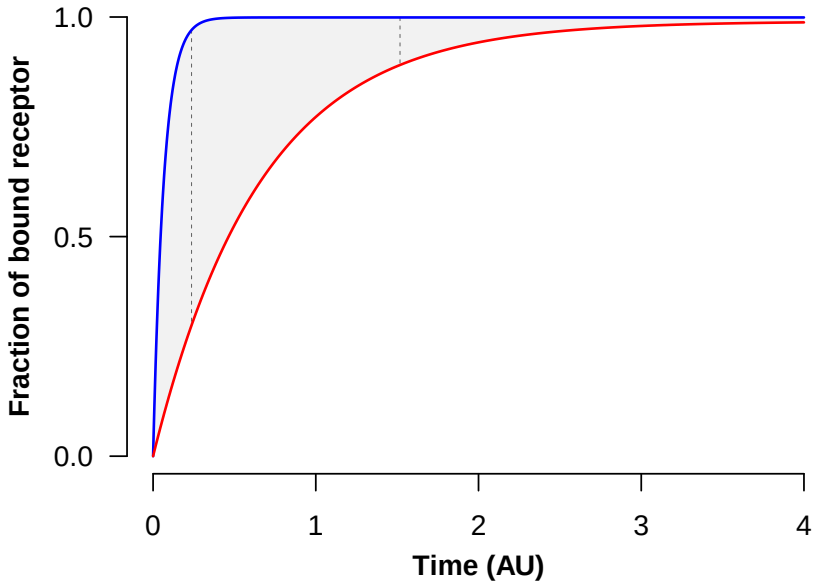

Figure 1.4: Different saturating ligand concentrations may be distinguishable before receptor binding reaches equilibrium. Binding of receptor over time for a high (blue curve) and a low (red curve) saturating concentration of ligand. In pre-equilibrium, the fractions of bound receptor differ greatly between the curves. This difference becomes progressively smaller as the reactions approach their equilibria. Dashed lines mark the difference in complex for the curves at two different time points.

inversely proportional to L, so that increasing the ligand concentration decreases the value of τ. When $\tau = t$, the exponential function in equation 1.2 equals $e^{-t/\tau} = e^{-1} = 0.368$, indicating that 63.2% of $\mathrm{R}_{\mathrm{tot}}$ are bound by ligand. $\tau = t$ is therefore defined as the characteristic time of the reaction. This means that a decrease in τ in response to increasing ligand, is equivalent to a decrease in the characteristic time, or the time it takes until 63.2% of the receptors are bound by ligand (Lipták, 2012).

This ligand-dependency of the time constant is what enables differential complex formation during pre-equilibrium, and is therefore of central importance for PrESS. More generally, PrESS requires the *response time* of the system—i.e., the time it takes to reach a predefined fraction of a complete response—is dependent on the level of input.

1.2.2 Pre-equilibrium information can be isolated through a downstream transient response

To further elaborate on the idea of PrESS, Ventura et al. (2014) reasoned that the response to pre-equilibrium information could be assisted by preventing signaling from occupied receptors once ligand binding has reached equilibrium. This would essentially extract only the pre-equilibrium information, while the uninformative equilibrium information is muted.

Through mathematical modeling the authors showed that such an effect could be achieved if the signaling response downstream of the receptors is transient. They exemplified this by developing three toy models, each representing a distinct architecture of a hypothetical downstream response, and placed these downstream of the activated complex in the ligand–receptor model. One of the designs, based around a negative feedback loop, is shown in figure 1.5a.

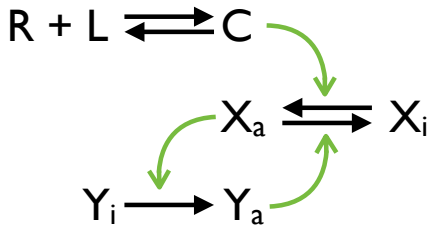

(a)

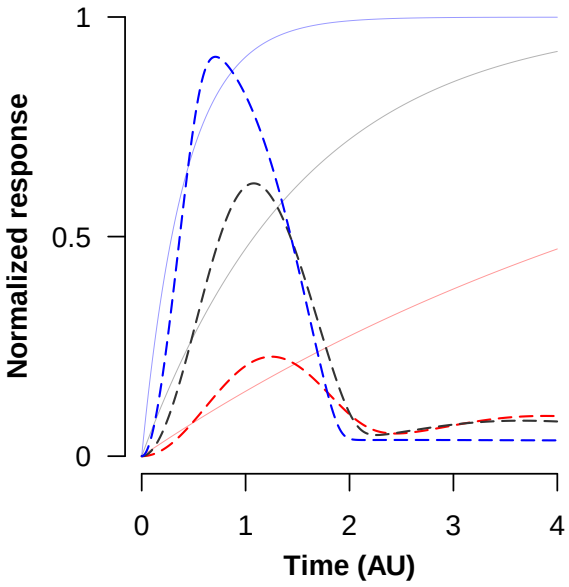

(b)

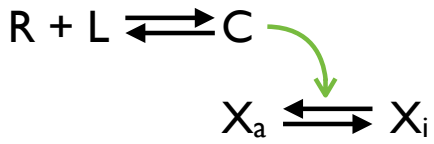

(c)

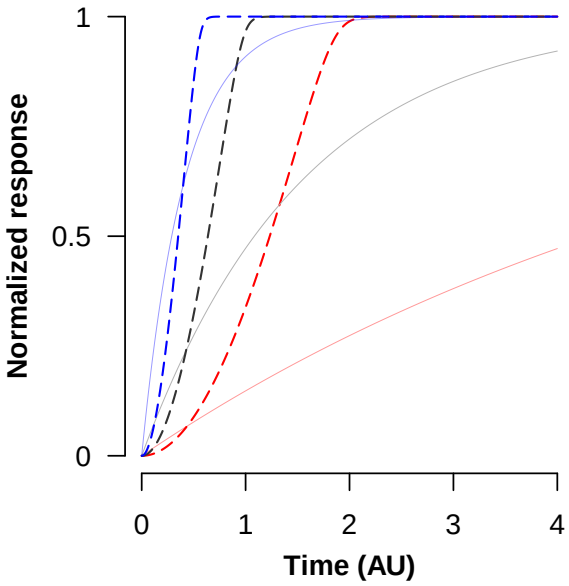

(d)

Figure 1.5: A transient response downstream of the activated receptor complex can isolate pre-equilibrium information. (a) Proposed design for a transient response based on a negative feedback loop. Subscripts a and i denote active and inactive molecules, respectively. **(b)** Modeling results of the design shown in (a). Accumulation over time is shown for activated complex (C; solid, faded lines) and active X (X_a; dashed, clear lines) for three different ligand concentrations (color coded). **(c)–(d)** Same as (a)–(b) with the feedback loop inactivated. Note that the downstream signaling rate (steepness of the dashed curves) depends on the fraction of formed complex. Figures and model adapted from Ventura et al. (2014).

Their results showed that transient signaling downstream of the activated receptor gives rise to a peak-like response, with the amplitude of the peak directly correlated with the ligand concentration in the ligand–receptor binding reaction. Furthermore, if the transient response is fast relative to ligand–receptor binding, signaling returns to nearly basal levels before the binding reaction has reached equilibrium, thereby avoiding the transmission of equilibrium information (figure 1.5b).

Thus, these results indicated that a transient response can assist PrESS by isolating the pre-equilibrium information.

1.3 A simple, controllable circuit for putting PrESS to the test

Although the idea of PrESS originally arose from studying the yeast pheromone response, its biological significance has yet to be demonstrated in practice. This is particularly true for the integration with a downstream transient response, as this is a purely conceptual idea.

Ventura et al. (2014) demonstrated through a combination of modeling and experiments that the pheromone response shows potential PrESS characteristics. However, the complexity of the signal transduction pathway downstream of the pheromone receptor makes it difficult to adapt as a model system for PrESS. Instead it was suggested that a simple genetic circuit be constructed, in which important parameters and components could be modified as required to generate the necessary dynamics for PrESS.

Based on this idea, the goal of this thesis project was to design, model, and biologically implement a controllable system in the form of a genetic circuit in yeast.

Chapter 2

Background

Setting the stage for PrESS

Following the idea of pre-equilibrium sensing and signaling (PrESS) introduced in the previous chapter, the goal of this project was to construct a synthetic signaling circuit capable of responding in PrESS mode. Given two different levels of input that both saturate their targets in equilibrium, the system should be capable of distinguishing between the inputs using differential information available before steady state. This system could serve as a proof of concept to show that the theoretical idea of PrESS can also function in practice.

This chapter describes some of the characteristics and features that were considered important for the circuit design, what approaches that were chosen for generating those characteristics, and how this led to the candidate systems that were eventually chosen as starting points for this project.

2.1 Transcriptional networks offer high plasticity and specificity

For any synthetic signaling system, of central importance is the ability to route signals to specific destinations, and to control the response at the sites of signal reception. By analogy with a directed network graph, this would be equivalent to selecting the connectivity of the edges and choosing the representation of each node (figure 2.1).

Since most signal propagation within a cell relies on the physical binding of two or more molecules, synthetic routing of signaling pathways is limited by the binding capabilities of the molecular species involved. Therefore, in order for a signaling molecule to produce a desired output, a minimum requirement is that the incoming signaling molecule can physically connect with the component(s) responsible for producing the desired response. However, the structural complexity of many signaling molecules makes it all but trivial to change their binding specificities. And although addition of specific binding domains could potentially provide proteins with docking sites for new interaction partners, binding alone is not necessarily sufficient for successful regulation of for example enzyme activity (Berg et al., 2012).

An interesting exception, where binding is generally sufficient for regulating a response, can be found in transcriptional regulation. Transcription factors (TFs) that bind directly to DNA carry specific

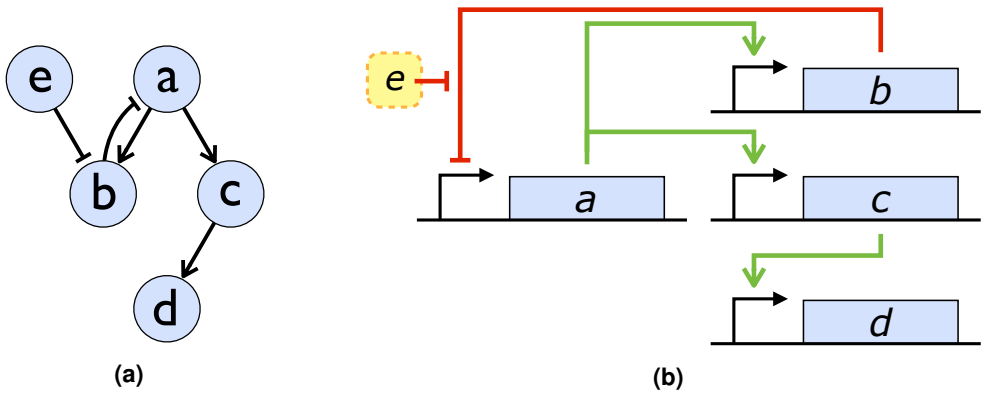

Figure 2.1: Transcriptional networks are good frameworks for synthetic cell signaling. (a) Example of a directed graph. Nodes denote molecular species, edges the influence of the source on its target. Arrowheads and tee-heads indicate positive and negative influence of biochemical activity, respectively. **(b)** Representation of the directed graph in (a) as a transcriptional network. Filled rectangles indicate genes and black arrows their promoters. Yellow box denotes a small, non-protein molecular ligand. Regulation of biochemical activity is indicated with green arrowheads (positive regulation) or red tee-heads (negative regulation).

DNA-binding domains that enable them to recognize and bind unique regulatory sequences in the promoters they regulate. Depending on the TF, the protein may also contain additional functional domains that defines its regulatory activity, such as a ligand binding domain that regulates the TF's regulatory activity in response to binding of a specific ligand, or—in the case of transcriptional activators—an activation domain (AD) responsible for recruiting components of the cell's transcription machinery (Hahn and Young, 2011).

For a functional TF, its gene regulation potential depends on its ability to bind the specific regulatory sequence in a target promoter. I.e., successful binding between TF and promoter is sufficient for regulating promoter activity. Since promoters can drive the expression of practically any protein coding gene, this means that a single, highly specific binding reaction between a TF–promoter pair can be coupled to a broad range of different outputs.

This ability to couple and regulate different inputs and outputs with high specificity gives the type of plasticity needed for enabling synthetic routing of signals, and thus make transcriptional networks good platforms for constructing synthetic signaling networks.

2.2 General properties and features

In order to give the transcriptional circuit the ability to operate in PrESS mode, some key properties are essential for generating the necessary dynamics. Other features may not be necessary for sensing and signaling, but may add desirable qualities for making the circuit experimentally useful.

2.2.1 Controlled timing and level of input

Since the main purpose of the circuit is to enable analysis of pre-equilibrium events in response to different levels of input, both the timing and level of input to the system need to be controllable. The circuit should respond to a specific and externally supplied input not intrinsic to the system. This ensures

Figure 2.2: Original proposal for a genetic circuit performing PrESS. .

that signaling cannot start prematurely and that the level of input is well defined.

For transcriptional networks such externally controlled inputs can be readily introduced through chemically controlled TFs. This type of induction can be used for activation as well as inactivation of gene expression, where the mode of regulation depends on the type of TF used and how it is implemented into the circuit (Gossen and Bujard, 2002; Lewis, 2005).

2.2.2 Input-to-dynamics conversion

As was described in chapter 1, a fundamental property required for PrESS signaling is the ability to convert different levels of input into different pre-equilibrium dynamics. In the simple ligand–receptor model described in section 1.2, this was achieved via the binding reaction between ligand and receptor, where the characteristic time constant τ (the time it takes to reach 63.2% of the steady state levels of bound receptor) decreased with increasing concentrations of ligand. Since this conversion is the enabling source of PrESS, any system capable of performing PrESS needs a *sensing mechanism* capable of emulating this type of input-to-dynamics conversion.

Whereas binding reactions are good sources for generating PrESS dynamics, not all binding reactions are sufficiently slow to yield a large enough pre-equilibrium time window (Ventura et al., 2014). .

2.2.3 Readily quantifiable dynamics and outputs

Easily measureable and quantifiable reporters are vital for the circuit to serve as a useful experimental system, as it enables continuous monitoring of the signaling dynamics. In the ideal case, all molecules and reactions contributing to PrESS can be followed simultaneously; including input to and output from the sensing mechanism, the dynamics of the transient response, and the overall system output.

2.3 Circuit design

In an early design, the transcriptional circuit shown in figure 2.2 was proposed as a potential system capable of performing PrESS. Here the *controllable input* is depicted by I; the *sensing mechanism* is represented by gene *a* and component X; the *transient response* is generated by genes *b* and *c*; and the *quantifiable output* is the product of gene *d*. .

The sought behavior of the circuit can be summarized as follows: . This yields the desired peak of the

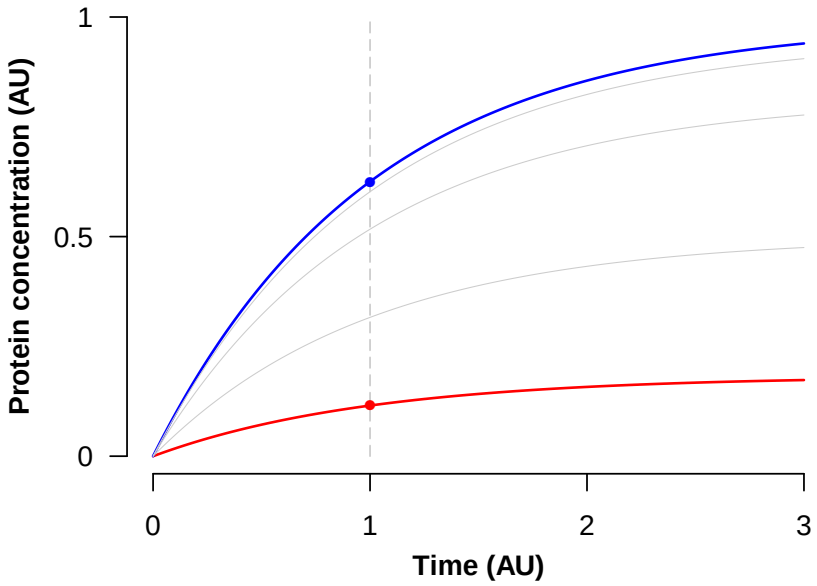

Figure 2.3: Regulation of protein synthesis rates does not shift the response time. Protein levels over time in response to different inputs. Input levels range from low (red curve) to high (blue curve), with the latter being saturating. Colored dots and vertical, dashed line indicate the response time, the time at which 63.2% of the protein levels in equilibrium is reached.

sought transient response. Gene ? serves as a control gene, showing that the level of input saturates the system at steady state.

As should be clear from the introduction to PrESS, the shape of the transient peak depends on the initial level of gene ? expression. When full (100%) expression is close to instant, high concentrations of the ?-encoded protein will accumulate before the levels drop. In contrast, when expression increases gradually (due to slow accumulation of the protein expressed by ?), or at expression levels below 100%, the expression of ? will be slower and result in a lower peak. Therefore, the ability to distinguish between different saturating concentrations of input depends on the ability of the sensing mechanism to convert these inputs into different dynamics in the expression of ?. This then affects ? transcription, and thus the expression peak.

2.3.1 Modeling revealed that varying the synthesis rate does not shift the response time

To test whether transcriptional activation can generate the necessary dynamics for PrESS, the proposed sensing mechanism was analyzed qualitatively by mathematical modeling based on a simple differential equation:

$$\frac{d\mathrm{A}}{dt} = \alpha \mathrm{F}(\mathrm{I}) - \beta \mathrm{A}. \tag{2.1}$$

Here parameters α and β denote the rate constants for synthesis and depletion of protein A, respectively. F is an input function representing promoter regulation, and receives different *static* inputs, I, that reflect different levels of inducer. The function approaches $\mathrm{F}(\mathrm{I}) = 1$ at high levels of input, reflecting maximal promoter activity.

The results revealed that this mechanism could not generate the necessary dynamics for PrESS.

That is, changing the concentration of inducer would not shift the response time of A (figure 2.3). This is an expected result, for the response time in protein dynamics does not depend on the production rate. Increasing the rate of synthesis results in higher protein concentrations at steady state, but it does not change the response time. This can be seen from the solution of equation 2.1:

$$\mathrm{A}_{(t,\mathrm{I})} = \mathrm{A}_{\mathrm{eq(I)}} \left(1 - e^{-t/\tau}\right) \tag{2.2}$$

$$\mathrm{A}_{\mathrm{eq(I)}} = \frac{\alpha}{\beta}\,\mathrm{F(I)} \tag{2.3}$$

$$\tau = \frac{1}{\beta} \tag{2.4}$$

In contrast to the ligand–receptor binding reaction, where the time constant τ was directly dependent on the level of input (section 1.2.1), this is not the case for protein synthesis, as τ is not dependent on the input function. More specifically, the synthesis rate constant α is not represented in the exponential function that describes the time evolution of protein A, and can therefore not affect its accumulation over time.

Thus, when promoter regulation is modeled by a function receiving *static* inputs, different levels of input will only affect the steady state levels of protein, whereas the time to reach these steady states will be constant. Put differently, for different saturating levels of input the protein dynamics will be identical, and cannot generate the pre-equilibrium dynamics necessary for PrESS (Alon, 2007).

While not synthesis dependent, the representation of β in equation 2.4 suggests that the protein response time is instead depletion dependent. This indicates that the sought PrESS dynamics could potentially be generated by letting the input directly regulate the protein depletion rate. However, instead of actively regulating protein depletion through degradation, it was suggested that the effect of depletion could be mimicked.

2.3.2 X–Y binding is a potential sensing mechanism

While exploring this idea, attention was turned towards a publication exploring effects of different genetic designs on gene expression. The authors constructed genetic circuits (chapter 4, figures 4.1a and 4.1b).

Through mathematical modeling and experimental results it was shown that.

The primary interest in these circuits for the sensing mechanism lay in the control of X. The regulatory activity of X can be blocked by Y. Y binds X with exceptionally high affinity and causes a conformational change that drastically decreases X's activity. Y essentially inactivates X and makes it *unavailable* for carrying out its activity.

Whereas this Y-induced X inactivation was originally proposed as a potential depletion mimic, the interest in this mechanism for this project took a different turn. Instead of utilizing Y for artificially regulating the halflife of X, it was thought that the binding reaction between X and Y could itself support a shift in response time, analogous to the previously described ligand–receptor binding reaction. However, in

contrast to ligand–receptor binding, which directly forms an active complex that participates in the downstream signaling, the output following X–Y binding is indirect. . It was therefore not obvious whether the input-dependent response times from X–Y binding would also be reflected gene expression.

Chapter 3

Materials and methods

Media and PrESS transparency

3.1 Yeast strains and growth media

Yeast used for experimental circuit analysis were kindly provided by the original authors. In short, these strains were derivatives of the haploid yeast *Saccharomyces cerevisiae*. See the original publication for further details. Yeast strain used for diffusion experiments was the W303a derivative ACL379 (genotype MATa, *leu2*-3,112, *trp*1-1, *can*1-100, *ura*3-1, *ade*2-1, *his*3-11,15, Δ*bar*1) (Colman-Lerner et al., 2005).

Yeast growth medium was a synthetic complete glucose-free medium with 2% galactose and 1% raffinose (SGR) (1.7 g/L yeast nitrogen base, 5 g/L ammonium sulfate, 0.79 g/L complete supplement mixture (MP Biomedicals), 2 mg/L adenine, 20 g/L D-galactose, 10 g/L D-raffinose).

3.2 Experimental procedures

3.2.1 Circuit 1 and circuit 2 steady state analyses

Circuit 1 or circuit 2 strains were inoculated in 5 mL SGR medium and grown at 30°C with agitation until early exponential phase. Cultures were then diluted 100 times in 5 mL fresh SGR and induced with inducer from 100 times concentrated stock solutions in 100% ethanol or with a 100% ethanol control solution. Cells were then allowed to grow in the same conditions for 16 h more until low cell densities ($\sim 10^{-8}$ cells/mL). Cells were harvested and protein translation was blocked by adding the protein biosynthesis inhibitor cycloheximide (Obrig et al., 1971; Schneider-Poetsch et al., 2010) to a final concentration of 25 μg/mL, from a 100 times concentration stock solution in 10% DMSO. Samples were kept at 4°C for 3 h to allow maturation of fluorescent proteins, after which cells were loaded in 384-well microplates for epifluorescence microscopy imaging (see section 3.2.4). Samples were loaded in duplicate wells, yielding two technical replicates per sample.

Fluorophore	Cube	Excitation	Dichroic	Emission
FP1	41004	HQ560/55x	Q595LP	HQ645/75m
FP2	41028	HQ500/20x	Q515LP	HQ535/30m
inducer	31044v2	D436/20x	455DCLP	D480/40m

Table 3.1: Filter cubes used for fluorescence microscopy experiments.

3.2.2 Circuit 1 and circuit 2 time course analyses

Circuit 1 and circuit 2 strains were inoculated in 5 mL SGR medium and grown at 30°C with agitation until early exponential phase. Cultures were diluted 100 times in 5 mL fresh SGR and allowed to continue growth until low cell densities ($\sim 10^{-8}$ cells/mL). Cultures were then again diluted 1:3 in 5 mL fresh SGR and cells allowed to adapt for 1 h before induction with inducer from 100 times concentrated stock solutions in 100% ethanol. Cultures were sampled at regular intervals over 9 h and protein translation was blocked with the protein biosynthesis inhibitor cycloheximide (Obrig et al., 1971; Schneider-Poetsch et al., 2010) to a final concentration of 25 μg/ml. Samples were kept at 4°C for 15–24 h to allow maturation of fluorescent proteins, after which cells were loaded in 384-well microplates for epifluorescence microscopy imaging (see section 3.2.4). Samples were loaded in duplicate wells, yielding two technical replicates per sample.

3.2.3 Inducer cell accumulation analysis

ACL379 yeast was inoculated in 5 mL SGR medium and grown at 30°C with agitation until early exponential phase. Cultures were diluted 100 times in 5 mL fresh SGR and allowed to continue growth until low cell densities ($\sim 10^{-8}$ cells/mL). Cultures were then again diluted 1:3 in 5 mL fresh SGR and cells allowed to adapt for 1 h before induction with inducer from 100 times concentrated stock solutions in 100% ethanol. Cultures were sampled at regular intervals over 5 h and immediately loaded in 384-well microplates for epifluorescence microscopy imaging (see section 3.2.4). Samples were loaded in duplicate wells, yielding two technical replicates per sample.

3.2.4 Fluorescence microscopy

Yeast cell imaging was performed by epifluorescence microscopy using an Olympus IX81 microscope with an Olympus UPlanSApo 60x/1.35 oil immersion objective. Cells were illuminated with LEDs centered at 510 nm (fluorescent proteins) or 440 nm (inducer) through microscope excitation/emission filter cubes as shown in table 3.1, and emission was measured for either 300 ms (fluorescent protein 2 (FP2) and inducer) or 500 ms (fluorescent protein 1 (FP1)). Imaging order was FP1, FP2, and inducer.

3.3 Computational analysis

3.3.1 Cell segmentation and quantification

Yeast cells were segmented and cell fluorescence was quantified using Cell-ID 1.4, an open-source software for segmentation and quantification of microscopy images of yeast cells (Bush et al., 2012). In short, Cell-ID first segments cell boundaries based on out-of-focus brightfield images. Fluorescence images are then overlaid with their corresponding segmentation masks, allowing single-cell quantification of image intensities corresponding to cell fluorescence.

3.3.2 Fluorescence and statistical analysis

Cell fluorescence quantification data were imported from Cell-ID 1.4 to the statistical analysis software R 3.0.2 (R Core Team, 2013). Background correction was carried out for all cells before statistical analysis by subtracting the background calculated by Cell-ID according to the formula:

$$\mathrm{F_{corr}} = \mathrm{F_{tot}} - \mathrm{A_{tot}} \times \mathrm{F_{bg}}, \tag{3.1}$$

where $\mathrm{F_{corr}}$ is the background corrected total cell fluorescence, $\mathrm{F_{tot}}$ is the original total cell fluorescence, $\mathrm{A_{tot}}$ is the total cell area in pixels, and $\mathrm{F_{bg}}$ is the mean background fluorescence per pixel calculated by Cell-ID.

Background corrected cell fluorescence data was used for all statistical analysis in R. Population fluorescence means and 99% confidence intervals were calculated with the bootstrapping technique described in the excellent article by Fay and Gerow (2013). In short, each sample was resampled with replacement 4000 times, calculating the population mean after each round. The 4000 calculated means were then sorted in a vector from lowest to highest, and sample mean as well as lower and upper 99% confidence interval values selected by taking the mean values for vector positions 2000–2001, 20–21, and 3980–3981, respectively. Standard deviations were calculated with the innate function `sd()` in R.

3.3.3 Plotting

All plotting was performed based on the innate `plot()` function in R 3.0.2.

3.4 Computational modeling

3.4.1 Circuit 1 and circuit 2 modeling

Computational modeling was performed in COPASI 4.11 (Build 65), a simulator for biochemical networks (Hoops et al., 2006). Mathematical models for circuit 1 and circuit 2 were adapted from the original publication (see appendix A) and implemented in COPASI based on equivalent biochemical reactions.

Initial states for time course analyses were obtained by running a `Steady State` task with all initial species concentrations preset to zero. Resulting steady state values were then set as initial species

concentrations. Time course analyses for different levels of input were performed in a `Parameter scan` task, subtask `Time course`, scanning `ye` logarithmically for initial concentrations in the ranges 230–5000 (circuit 1) or 350–5000 (circuit 2). Time course durations were either 1, 5, or 20 hours (see main text) at 1000 intervals. Results were output to plots of transient concentrations of species `x` or `z` over `Model Time`. Plotting data was then saved for replotting in the statistical analysis software R 3.0.2 (R Core Team, 2013).

3.4.2 Modeling of the effect of slow inducer diffusion on X–Y binding

The effect of slow inducer diffusion on X–Y binding was modeled in COPASI loosely based on the circuit 1 and circuit 2 models. Assuming no synthesis nor dilution of ?, the model was implemented using biochemical reactions where parameter values were the same as for circuit 1 and circuit 2. Variable `?` was fixed to reflect a situation where the extracellular concentration is not affected by the diffusion reaction. Initial `?` value (intracellular inducer) was set to zero.

Inducer diffusion and X–Y binding were followed over time in a `Parameter scan` task, subtask `Time course`, scanning variables `?` and `?`. `?` was scanned for initial concentrations 300 and 600; and `ye` for initial concentrations 300 and 800. Time course duration was set to 5 hours at 1000 intervals. Results were output to plots of transient concentration of species `?` or `?` over `Model Time`. Plotting data was then saved for replotting in the statistical analysis software R 3.0.2 (R Core Team, 2013).

Chapter 4

Results

The importance of being slow on the uptake

While the transcriptional circuits described in the original publication have been extensively characterized both theoretically and experimentally by the original authors, their analyses were focused on the circuits' steady states. To test their performance as sensing mechanisms, the analyses needed to be expanded to uncover their pre-equilibrium dynamics.

Since the binding reaction between X and Y is present in all circuits, it was initially thought that X–Y binding dynamics would be similar for the circuit 1 and circuit 2 designs. It was also believed that the unique qualities of circuit 1 could later benefit the downstream transient response. This led the analysis to initially focus on circuit 1.

4.1 X–Y binding reaches equilibrium too fast to support PrESS in circuit 1

To investigate the potential of circuit 1 to generate the necessary pre-equilibrium dynamics, we were interested in studying the dynamics of X–Y binding upon exposing the system to different concentrations of Y. However, since binding of Y to X does not affect the cellular localization of X, we had no means of distinguishing between free and bound X. Therefore, X–Y binding could not be observed experimentally.

To get at least a qualitative measure of the potential of X–Y binding to support PrESS, the pre-equilibrium dynamics of the system were studied computationally. For this analysis, the mathematical model for circuit 1 developed by the original authors was adapted (figure 4.1a). This model, as well as that for circuit 2, had proven accurate in predicting the circuit's steady state dose-response behavior, and was therefore considered a good starting point also for the pre-equilibrium analysis. Furthermore, its relative simplicity made reimplementation straightforward.

Computational analysis was performed numerically in COPASI, a software for simulating biochemical networks (Hoops et al., 2006). Using the original parameter values from the original publication, the models were implemented as sets of biochemical reactions to precisely correspond to the three differ-

(a) Circuit 1

$$\frac{dX}{dt} =$$
$$\frac{dY}{dt} =$$
$$\frac{dZ}{dt} =$$

(b) Circuit 2

$$\frac{dX}{dt} =$$
$$\frac{dY}{dt} =$$
$$\frac{dZ}{dt} =$$

Figure 4.1: Visual representations and models for circuits 1 and 2. Variables X, Y, and Z represent X,Y, and Z, respectively. See appendix A and original publication for further details on models.

ential equations of the circuit 1 model (see Materials and methods, section 3.4). Starting concentrations for X (X) and the output Z (Z) were then obtained by running the model until steady state with the input kept constant at 0. This represented the state of the system before exposure to any Y. Finally, the range of inputs that led to maximal or near-maximal ($> 97\%$) concentrations of Z at steady state were identified. These input levels were regarded as saturating the system. Dynamics of X–Y binding in response to input were analyzed by following X over time for five different saturating levels of inputs. The results are shown in figure 4.2a, where X has been plotted over one hour in response to each input. Response times for 90% X binding relative to steady state levels have been marked for the highest and lowest inputs tested. These indicate that the response time of X decreases with increasing levels of input, which are precisely the dynamics required for PrESS. This effect is also highlighted in figure 4.2b, where the difference in X levels between the highest and lowest inputs in figure 4.2a is plotted over time. This shows that the difference in X concentrations quickly reaches a maximum, after which it decreases towards a steady state value where the difference in X–Y binding levels is constant. In other words, this peak represents the pre-equilibrium information that may help the system differentiate between inputs that are indistinguishable in equilibrium.

To see how the shift in response time of X reflects on Z, the production of Z was plotted over time for the same inputs as above (figure 4.3a). Although this plot indicates that the differential binding dynamics of X are also detectable in the expression dynamics of Z, this effect disappears when time scales are increased to 20 hours (figure 4.3b). It here becomes clear that the differential expression of Z following the pre-equilibrium dynamics of X is progressively lost to, yielding a result that resembles that predicted for a static input (figure 2.3, section 2.3.1). These results are not necessarily biologically relevant, since the deterministic nature of the model discerns even biologically negligible differences in X levels. Nevertheless, the slow response time of Z in relation to X–Y binding suggested that the biochemical processes involved may limit the ability to propagate upstream pre-equilibrium information.

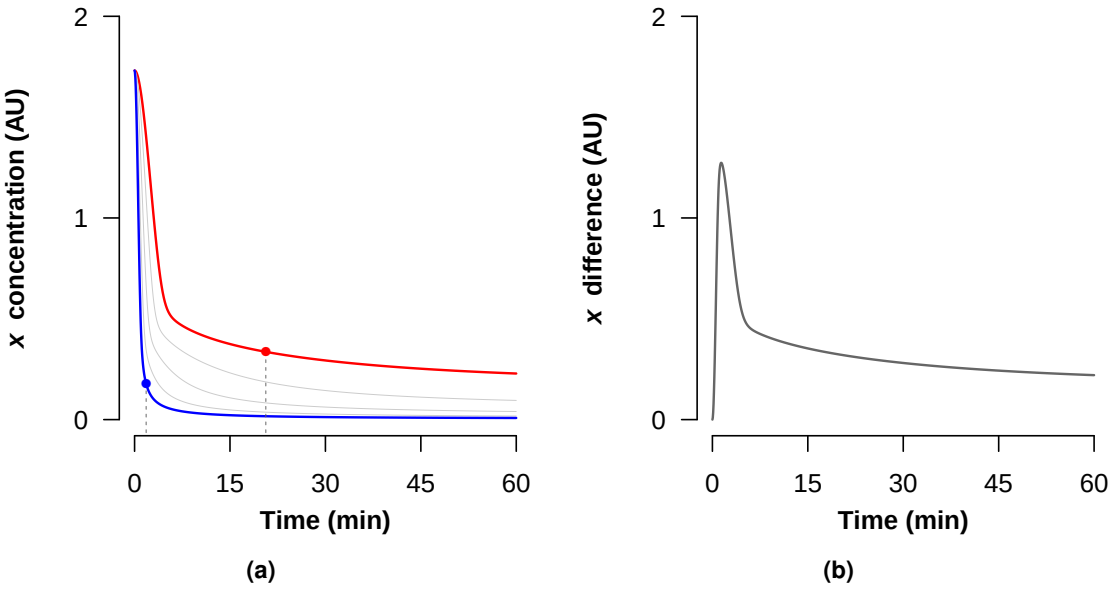

Figure 4.2: The response time of X binding in the circuit 1 model is input-dependent. (a) X is plotted over time in response to different saturating levels of input. Dots mark 90% binding relative to steady state X levels and indicate that response times are shorter at high inputs (blue line) than at low (red line). **(b)** Differences in X levels between the low and high inputs in (a) plotted over time.

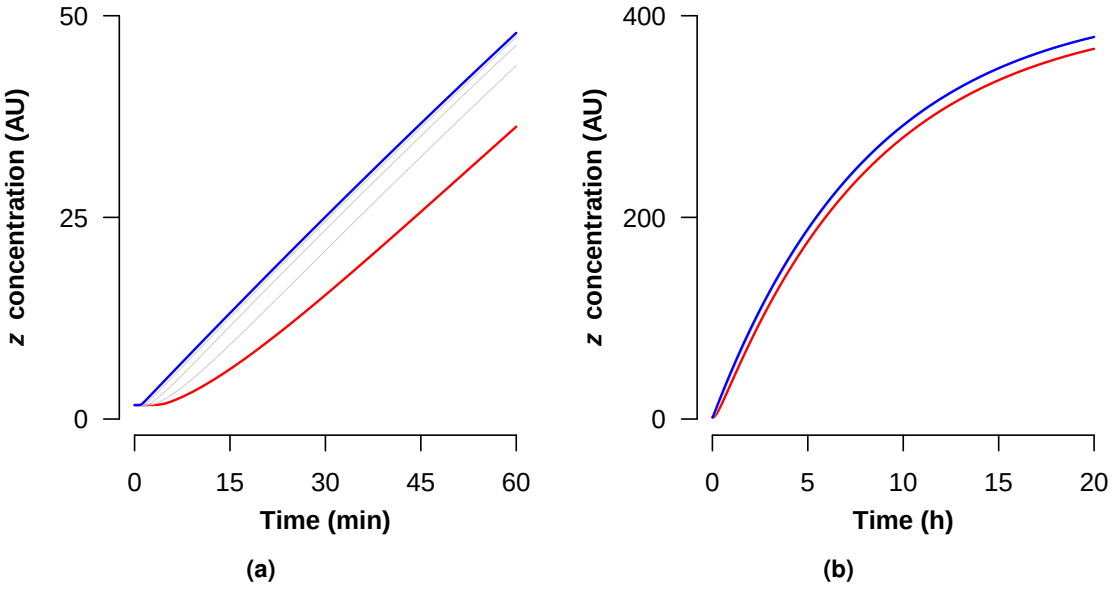

Figure 4.3: Binding dynamics of X do not significantly change the response time of Z in circuit 1.

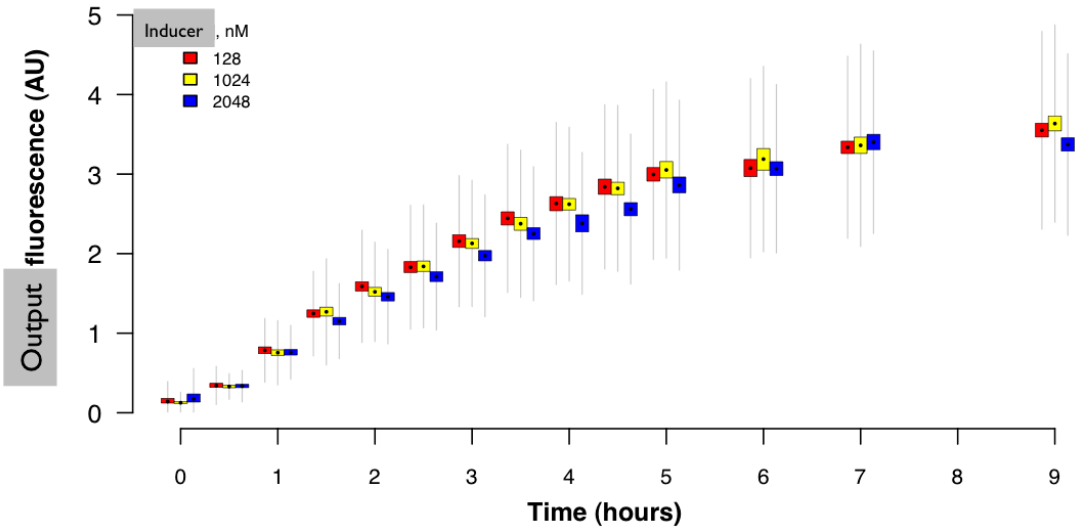

Figure 4.4: Circuit 1 output response times are not input-dependent. Fluorescent reporter in circuit 1 yeast monitored over nine hours in response to different saturating concentrations of inducer. Increasing input levels do not appear to decrease response times. Boxes span 99% confidence intervals around sample means, and whiskers show the standard deviation of each sample. Results from a single experiment, with sample sizes typically ranging between 100–1000 cells.

To verify the modeling results experimentally, a yeast strain representing an implementation of circuit 1 was used; see section 3.1). In short, this strain.

Expression dynamics in response to induction were studied by exposing cells to three diverse but saturating concentrations of inducer (figure B.1a). Reporter expression was then followed over nine hours by quantitatively measuring Z fluorescence in sampled populations of cells. In concordance with the model predictions, no consistent differences in Z fluorescence could be measured in response to the varying levels of inducer (figure 4.4). This does not necessarily mean that the system is incapable of producing the necessary PrESS dynamics, as differential expression could be in effect early in the response. However, the experimental setup was not sufficiently sensitive to capture any such dynamics. In fact, the results suggested a slight decrease in Z at the highest concentration. This is possibly initial signs of inducer toxicity, as it had been observed that concentrations of inducer above 2048 nM had a negative effect on cell growth.

While some attempts were made to improve experimental sensitivity via single-cell analysis, these analyses proved incompatible with the circuit 1 fluorescence reporter system (see appendix C). It was thereby concluded that circuit 1 could not be a useful sensing mechanism for PrESS.

4.2 Slow diffusion of inducer slows down binding reaction

During the experimental analysis of the circuit 1, it was observed that inducer accumulation in cells could be monitored by fluorescence microscopy. This revealed that inducer diffusion across the plasma membrane is remarkably slow, reaching equilibrium almost four hours after initial exposure (figure 4.5). Although this is not a new discovery, this unexpected realization significantly influenced the continuation of the project.

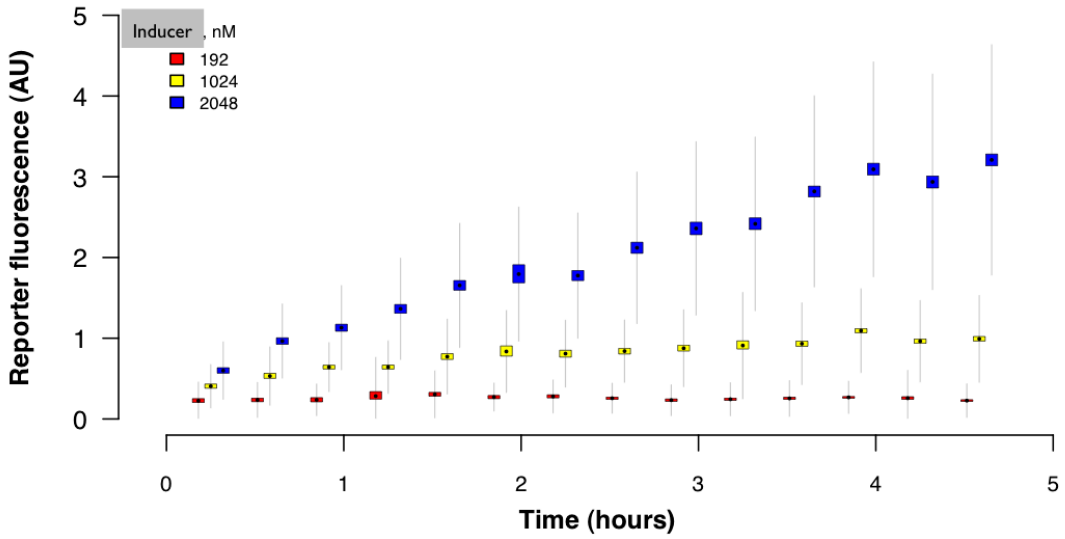

Figure 4.5: Inducer accumulation in yeast cells is slow. Accumulation of inducer in yeast was monitored by cell fluorescence over five hours after exposure, indicating that diffusion reaches equilibrium after approximately four hours. Boxes span 99% confidence intervals around sample means, and whiskers show the standard deviation of each sample. Results from a single experiment, with sample sizes typically ranging between 300–3000 cells.

An important consequence of slow inducer diffusion is that the availability of Y may become a limiting factor for the binding of Y to X. If the supply of Y to the reaction is much slower than the binding of Y to X, any Y that diffuses into the cell will quickly be absorbed by unbound Y molecules, until the point when practically all free X molecules have been bound by Y; only then will the concentration of free Y in the cell be allowed to increase. This means that the effective concentration of Y in the cell during binding of X is close to zero.

Recall from chapter 1, section 1.2 that the *forward* reaction in a simple binding reaction is proportional to the binding reaction rate constant, k_{on}, and the concentration of the reactants, X and Y:

$$X + Y \underset{k_{off}}{\overset{k_{on}}{\rightleftharpoons}} X{\cdot}Y \qquad \text{(R 4.2)}$$

For a given set of initial concentrations of Y and X, this reaction will approach a unique chemical equilibrium defined by the reaction rate constants k_{on} and k_{off}. If no restrictions are put on the availability of the reactants, the response time of the reaction will directly depend on the reaction rate constants and the *initial* concentrations of the reactants. On the contrary, if one of the reactants (in this case Y) is supplied at a rate slower than the binding reaction rate, the forward reaction will be continuously impeded by the lack of available reactant. As long as the final concentration of Y inside the cell is the same as for the unrestricted reaction, the same binding equilibrium will eventually be reached. However, the response time will have dramatically increased.

The fact that diffusion of inducer limits the X binding reaction rate essentially makes X–Y binding directly proportional to the rate of inducer influx. In addition, since the influx of inducer is proportional to the extracellular concentration of the molecule (Berg, 1993), the rate at which inducer accumulates could be controlled via the concentration of inducer in the growth medium. If the concentrations selected

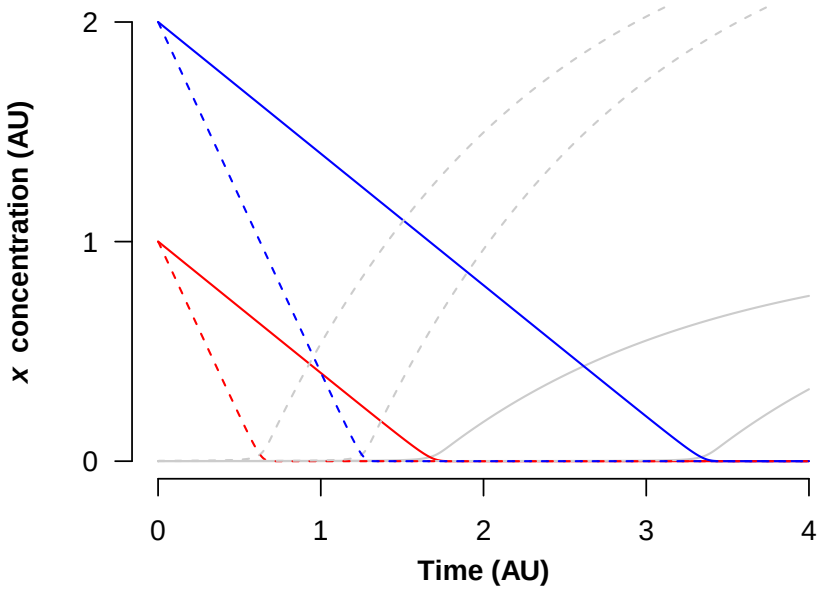

Figure 4.6: Initial X levels influence binding response times.

are saturating, their distinct rates of diffusion will be reflected by the time it takes for X to be completely bound, and thereby the generation of output. This is essentially a shift in response time where the time scale is defined by the diffusion rate constant rather than binding reaction rate constants (figure 4.6).

For a given inducer concentration, the time until complete X binding is strongly dependent on the initial X levels in the cell. The more X present before induction, the more time will elapse before enough inducer has diffused into the cell to bind all X. Consequently, since different concentrations of inducer give rise to different rates of X binding, larger initial pools of X will expand the difference in response times between the inducer concentrations (figure 4.6). This is an important difference compared to a non-diffusion limited binding reaction: since X is one of the reactants, increasing X concentrations will *decrease* the response time. In contrast, in the diffusion limited case, the increased reaction rate due to higher levels of X gets dominated by the slow supplementation of inducer.

In circuit 1, only low levels of X are present in the absence of inducer. Following the discussion above, it is possible that these levels may be too low for the system to take advantage of slow inducer diffusion. This could explain why no difference in Z could be measured for different inducer concentrations. However, it was hypothesized that the higher X levels in circuit 2 could be enough to support a diffusion-generated time response.

4.3 High initial X levels enables PrESS in circuit 2

To test the validity of this hypothesis, the computational analysis previously performed for circuit 1 was repeated for circuit 2. As before, model and parameter values were adapted from the original publication via the corresponding biochemical reactions in COPASI. Furthermore, although this was not considered for the analysis of circuit 1, the implementation of diffusion in the circuit 1 and 2 models was verified to correspond well with what had been observed experimentally by fluorescence microscopy. The model

also indicated a more than 300-fold increase in pre-induction levels of X. This high increase in X levels was later also observed experimentally (compare figures B.1b and B.2b).

As in the circuit 1 analysis, X binding was studied over time in response to highly diverse but saturating levels of input. The results are presented in figure 4.7a and show that the high levels of X in the system prior to induction results in binding dynamics markedly different from those seen for circuit 1, with response times ranging from minutes to several hours. This is also reflected in the output Z, whose onset is well timed with the complete binding of X (figure 4.7b). Importantly, the differences in Z concentrations between different levels of induction are larger earlier in the response, after which they progressively become smaller as Z levels approach steady state.

Modeling results were verified experimentally in yeast implementing circuit 2.

System response to induction was analyzed as previously described for circuit 1. Cells were induced with different saturating concentrations of inducer (figure B.2a), after which output fluorescence was monitored by sampling cells regularly over nine hours. Results agreed well with the qualitative modeling results for Z dynamics. Z accumulation in response to the lowest (192 nM) inducer concentration was clearly differentiable from that of the two higher concentrations (1024 nM and 2048 nM) (figure 4.8). This differentiation was the result of the 90-minute delay in the onset of output between the inputs. This delay could potentially be extended even further by choosing a lower but still saturating concentration of inducer, as shown in figure B.2a.

These results indicate that X–Y binding regulated by a slow-diffusing chemical inducer could potentially be a useful sensing mechanism for generating the necessary dynamics for PrESS.

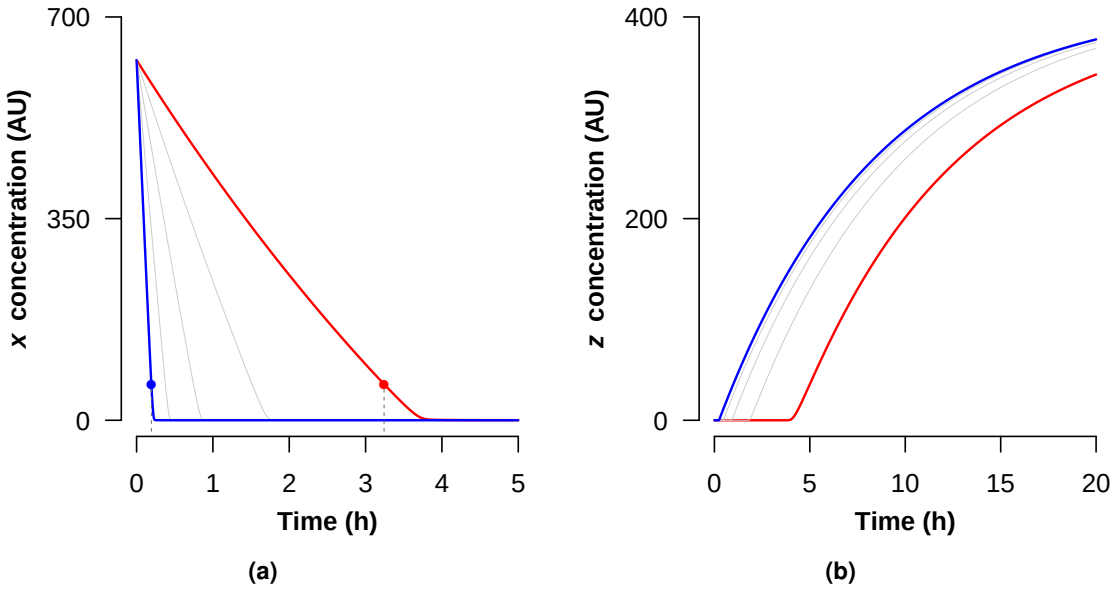

Figure 4.7: Slow X binding in circuit 2 shifts the response time of Z. (a) X binding is plotted over 5 hours for different saturating inputs. Dots marking 90% binding show a great shift in response times between high (blue line) and low (red line) inputs. **(b)** Output fluorescence over 20 hours for the inputs from (a), indicating that X binding dynamics are reflected also in the output.

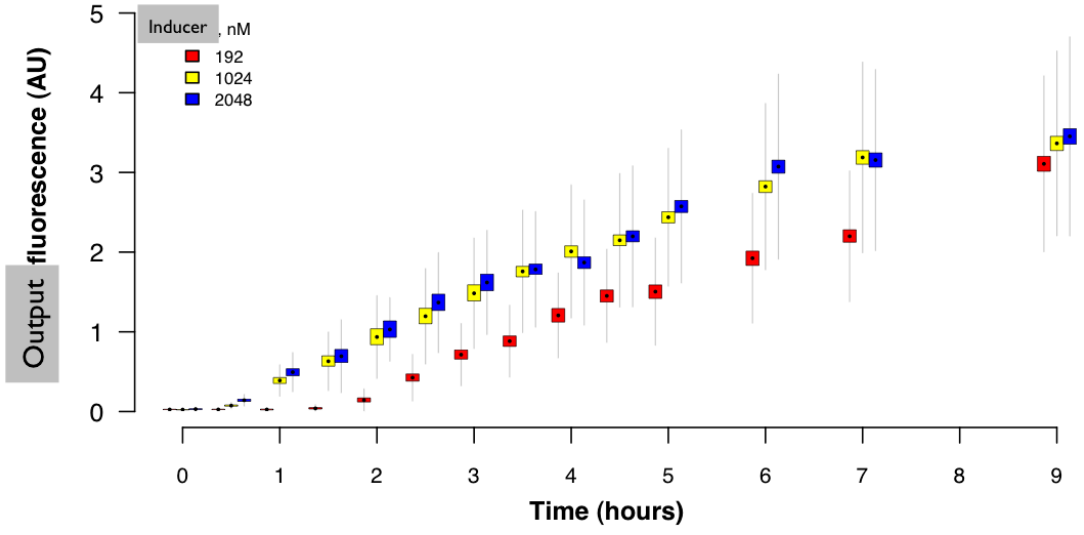

Figure 4.8: Circuit 2 output response times are input-dependent. Output fluorescence in circuit 2 yeast was monitored over 9 hours in response to different saturating concentrations of inducer. At high concentrations of inducer (1024–2048 nM) output starts accumulating almost immediately, similar to the results from circuit 1 yeast. In contrast, a lower concentration (192 nM) delays the onset of expression with over an hour. Boxes span 99% confidence intervals around sample means, and whiskers show the standard deviation of each sample. Results from a single experiment, with sample sizes typically ranging between 100–1000 cells.

Chapter 5

Discussion

Closer to success, but a long road PrESS

When X–Y binding was initially proposed as a potential sensing mechanism, it was thought that the binding reaction could yield pre-equilibrium dynamics similar to those of the ligand–receptor model. Doubts were instead raised for whether the biochemical reactions involved in signal propagation—the output equivalent to signaling from the activated receptor complex—would be fast enough to retain these pre-equilibrium dynamics. While the results show that circuit 2 can indeed propagate pre-equilibrium information, the mechanism by which this is achieved differs from that of the ligand–receptor model, resulting in dynamics distinct from those originally sought.

This work led to the following conclusions:

- Circuit 2 dynamics may alter the dynamics of the transient response
- XYZ-based sensing may be a better choice for PrESS
- Artificial depletion may circumvent some limitations of X–Y binding

The discoveries and experiences made during the course of this project have given valuable support for the use of a transcriptional network as a potential framework for synthetic implementation of PrESS. It has also highlighted several limiting factors that may complicate this implementation, in particular parameters that cannot easily be tuned and thereby set the experimental boundaries for the system.

It is important to note that successful implementation of PrESS does not depend on shifting the response times alone, but also on the implementation of downstream transient response. However, the time limitations of this master's thesis project did not allow for such implementations, but will be a challenge for the future.

Bibliography

Alon, U. (2007). *An introduction to systems biology: design principles of biological circuits*, chapter 2, pages 18–22. Chapman & Hall/CRC, Boca Raton.

Berg, H. C. (1993). *Random walks in biology*. Princeton University Press.

Berg, J. M., Tymoczko, J. L., and Stryer, L. (2012). *Biochemistry*, chapter 10, pages 289–314. W.H. Freeman, New York, 7 edition.

Bush, A., Chernomoretz, A., Yu, R., Gordon, A., and Colman-Lerner, A. (2012). Using Cell-ID 1.4 with R for microscope-based cytometry. *Curr Protoc Mol Biol*, Chapter 14:Unit 14.18.

Colman-Lerner, A., Gordon, A., Serra, E., Chin, T., Resnekov, O., Endy, D., Gustavo Pesce, C., and Brent, R. (2005). Regulated cell-to-cell variation in a cell-fate decision system. *Nature*, 437(7059):699–706.

Fay, D. S. and Gerow, K. (2013). A biologist's guide to statistical thinking and analysis. *WormBook*, pages 1–54.

Gomperts, B. D., Kramer, I. M., and Tatham, P. E. (2009). *Signal Transduction*, chapter 2, pages 21–35. Academic Press, 2, revised edition.

Gossen, M. and Bujard, H. (2002). Studying gene function in eukaryotes by conditional gene inactivation. *Annu Rev Genet*, 36:153–73.

Hahn, S. and Young, E. T. (2011). Transcriptional regulation in *Saccharomyces cerevisiae*: transcription factor regulation and function, mechanisms of initiation, and roles of activators and coactivators. *Genetics*, 189(3):705–36.

Hoops, S., Sahle, S., Gauges, R., Lee, C., Pahle, J., Simus, N., Singhal, M., Xu, L., Mendes, P., and Kummer, U. (2006). COPASI—a COmplex PAthway SImulator. *Bioinformatics*, 22(24):3067–74.

Lewis, M. (2005). The *lac* repressor. *C R Biol*, 328(6):521–48.

Lipták, B. G. (2012). *Instrument engineers' handbook*, volume Process Control and Optimization, page 100. CRC Press, Boca Raton, FL, 4 edition.

Moore, T. I., Chou, C.-S., Nie, Q., Jeon, N. L., and Yi, T.-M. (2008). Robust spatial sensing of mating pheromone gradients by yeast cells. *PLoS One*, 3(12):e3865.

Obrig, T. G., Culp, W. J., McKeehan, W. L., and Hardesty, B. (1971). The mechanism by which cycloheximide and related glutarimide antibiotics inhibit peptide synthesis on reticulocyte ribosomes. *J Biol Chem*, 246(1):174–81.

R Core Team (2013). *R: A language and environment for statistical computing*. R Foundation for Statistical Computing, Vienna, Austria.

Schneider-Poetsch, T., Ju, J., Eyler, D. E., Dang, Y., Bhat, S., Merrick, W. C., Green, R., Shen, B., and Liu, J. O. (2010). Inhibition of eukaryotic translation elongation by cycloheximide and lactimidomycin. *Nat Chem Biol*, 6(3):209–217.

Segall, J. E. (1993). Polarization of yeast cells in spatial gradients of alpha mating factor. *Proc Natl Acad Sci U S A*, 90(18):8332–6.

Stock, A. M., Robinson, V. L., and Goudreau, P. N. (2000). Two-component signal transduction. *Annu Rev Biochem*, 69:183–215.

Ventura, A. C., Bush, A., Vasen, G., Goldín, M. A., Burkinshaw, B., Bhattacharjee, N., Folch, A., Brent, R., Chernomoretz, A., and Colman-Lerner, A. (2014). Utilization of extracellular information before ligand-receptor binding reaches equilibrium expands and shifts the input dynamic range. *Proc Natl Acad Sci U S A*, 111(37):E3860–9.

Appendix A

Model adaptation

Appendix B

Dose–response curves

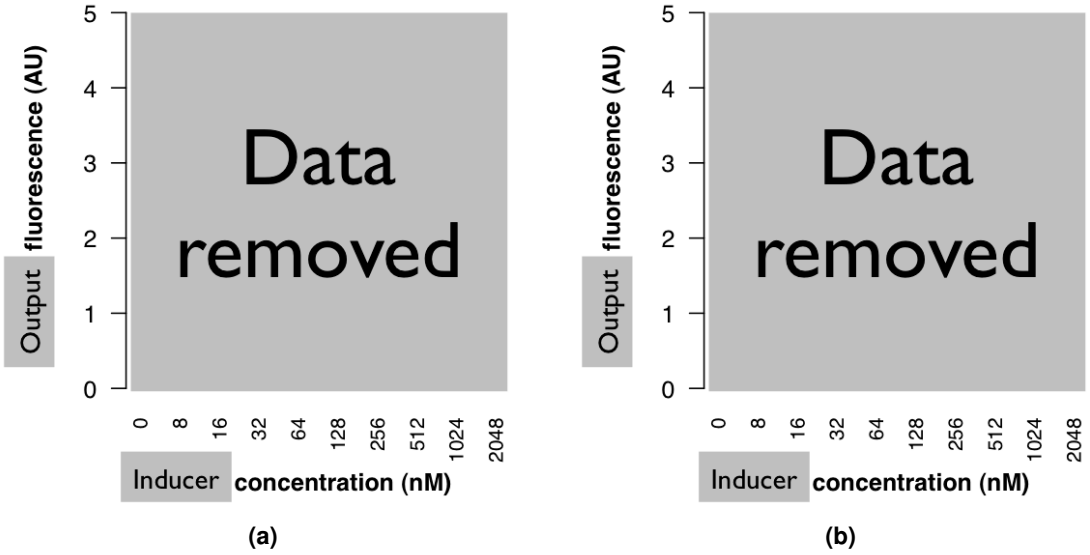

Figure B.1: Steady state dose response curves used to determine saturating or nearly saturating inducer concentrations for the circuit 1 strain.

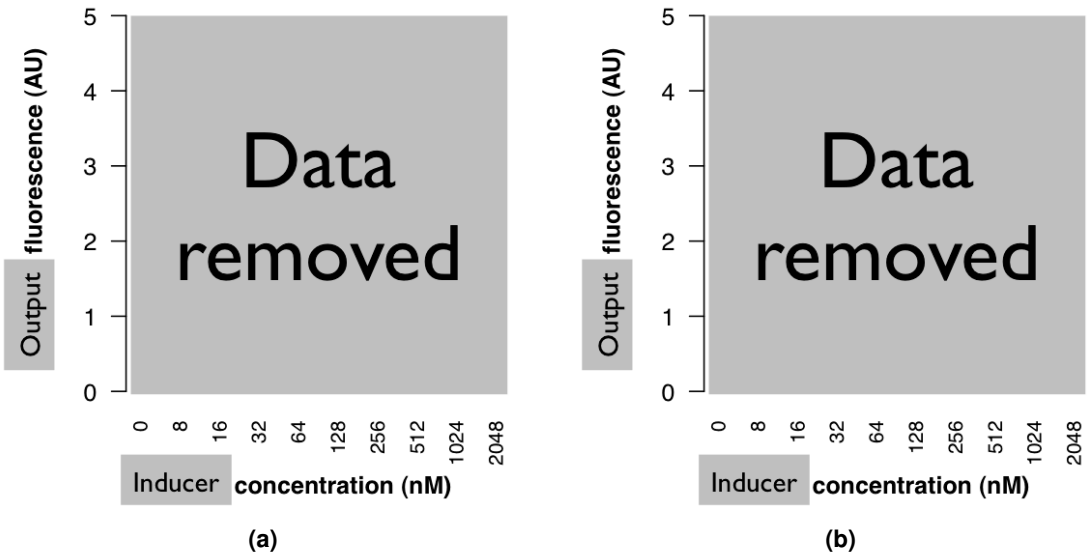

Figure B.2: Steady state dose response curves used to determine saturating or nearly saturating inducer concentrations for the circuit 2 strain.

Appendix C

Single cell analysis